An optical sensor for monitoring of dissolved oxygen based on phase detection

Weiwei Feng[1,2], Na Zhou[1,2], Lingxin Chen[1,2,3] and Bowei Li[1]

[1] Key Laboratory of Coastal Zone Environmental Processes and Ecological Remediation, Yantai Institute of Coastal Zone Research, Chinese Academy of Sciences, Yantai 264003, People's Republic of China
[2] Costal Environment Engineering Technology Research Center of Shandong Province, Yantai 264003, People's Republic of China

E-mail: wwfeng@yic.ac.cn and lxchen@yic.ac.cn

Abstract

Dissolved oxygen (DO) monitoring is of vital importance to water treatment, sewage treatment, aquaculture and biological research. The traditional method for DO detection is an electrochemical method called the Clark electrode. This electrochemical method has been widely used as it is simple and inexpensive; however, the critical drawback for this kind of sensor is that it is easily affected by pH variations, and by the concentration of H_2S and SO_2. Optical sensing for DO detection is a newly developed technology, which can avoid most of the drawbacks of the electrochemical sensors. A DO sensor using fluorescence detection is described in this paper. The oxygen concentration measurement principle is based on optical phase detection, which is more precise than the traditional intensity detection method. Emission is carried out by a low-cost, specially designed light emitting diode (LED) source. To avoid an unwanted phase shift, a reference LED is used to improve the degree of accuracy. The sensing material for fluorescence is a ruthenium complex. A discrete Fourier transform (DFT) algorithm was used for the phase calculation. The system was designed into a stainless steel probe, and dissolved oxygen concentration measurement results for various applications are presented in this paper.

Keywords: optical sensor, luminescence quenching time, phase detection, dissolved oxygen

(Some figures may appear in colour only in the online journal)

1. Introduction

The determination of dissolved oxygen (DO) concentration is of great importance in many areas of industry, environmental control and biological research. Also, the amount of DO can be directly used to indicate water quality. A decrease in this amount usually indicates the presence of pollution. Under a standard atmospheric pressure of 101.325 kPa, the concentration of oxygen in water is 9.2 ppm at 20 °C. For most species of fish, the DO concentration should not fall under 5 ppm, otherwise they can hardly survive for the lack of oxygen. Additionally, in biological research, it is very important to monitor DO levels in blood, for blood is the transport medium for oxygen to cells and tissues throughout the body. Hence, we could obtain much valuable information about human health from the DO levels of blood.

Traditionally, there are two major techniques employed to detect DO, the Winkler method [1] and the amperometric method [2]. The Winkler method requires cumbersome steps, large sample volumes and is not suitable for rapid detection. The amperometric method is an electrochemical method which is called the Clark electrode; this method is very fast, but consumes the oxygen of the analyte in an electrochemical reaction and is easily corroded. For this reason, this method is not suitable for operation in long-term corrosive environments. Optical sensors have been gradually introduced into environmental monitoring, having the advantage of electromagnetic immunity, electrical isolation and a wide dynamic range. Compared with electrochemical methods, optical dissolved oxygen sensors

---

[3] Author to whom any correspondence should be addressed.

have attractive advantages in that they never consume oxygen and are resistant to corrosion [2–6]. Therefore, optical methods are more attractive than electrochemical methods. Ruthenium compounds are very attractive oxygen-sensing materials because of their long lifetime, strong absorption in the blue-green region of the spectrum, and large Stokes shift [7–11]. The dye of ruthenium compounds was entrapped into a microporous, hydrophobic sol–gel-derived cage-like microstructure that retains oxygen molecule permeability. When the dye reacts with oxygen, the fluorescence of the dye can be rapidly quenched. As the quenching time is proportional to the oxygen concentration, when the emitted light is modulated using a square signal, the phase shift of the fluorescence will also be proportional to the oxygen concentration. Hence we can use the phase information of the fluorescence to represent the oxygen concentration.

In this paper, a measuring instrument based on the above optical principle is presented. Two LED systems were used as the emitting system, and a discrete Fourier transform (DFT) algorithm was used for the phase calculation. The system was designed into a stainless steel probe, and dissolved oxygen concentration measurement results are presented in this paper.

2. Experimental section

2.1. Instruments

A LCQ Fleet LC-MS System (Thermo Fisher Scientific) was used to collect mass spectra. Elemental analyses were obtained with a Vario MACRO cube element analyzer. ^{1}H NMR, ^{13}C NMR spectra were taken on a Bruker spectrometer.

2.2. Materials

Dichloro(*p*-cymene)ruthenium(II)dimer, 4,7-diphenyl-1,10-phenanthroline, tetraethoxysilane (TEOS) and methyltri-ethoxysilane (MTEOS) were purchased from Aldrich. $Ru(Ph_2phen)_3Cl_2$ was synthesized and purified as described in the literature [12]. All other reagents and chemicals were from commercial sources and of analytical reagent grade, and used without further purification. Ultrapure water (Millipore, Bedford, MA, USA) was used throughout the experiment.

2.3. Sol–gel process and film fabrication

Sol–gel-derived silica films were fabricated from silicon alkoxide precursors, which undergo hydrolysis and poly-condensation reactions. Temperature controls the densification process [13]. If the temperature is less than 200 °C, a non-densified porous glass matrix is formed. This microporous glass acts as a support matrix for the analyte-sensitive dyes containing ruthenium compounds that are later added to the silicon alkoxide solution. Dye molecules are entrapped into nanometer-scale cages formed by the cross-linking silicon and oxygen units. Smaller analyte molecules can permeate the matrix and access the dye complex within the pores. By selecting fabrication parameters appropriate to the size of the dopant, molecule leaching is negligible [14].

The process of film fabrication includes mixing a silicon alkoxide precursor with ethanol, water and hydrochloric acid.

The precursors used for the sol–gel preparation in this work were TEOS and MTEOS. The ruthenium complex is added to the precursor solution, which is then stirred for 6 h at room temperature. The concentration of the ruthenium complex was 2–3 mg ml^{-1} with respect to the precursor solution. After stirring, the sol was stored at 70 °C for 12 h to promote hydrolysis and condensation polymerization. Then, the sol was dip-coated into a draft-free environment on these glass plates using a dip-coating apparatus. Before coating, these glass plates were soaked for 24 h in concentrated nitric acid, and then cleaned sequentially using de-ionized water, methanol and further de-ionized water. After dip-coating, the films were then finally dried for 18 h at 45 °C [15].

2.3.1. Synthesis of the ruthenium complex. The complex was synthesized in a commercial microwave oven (CEM, Discover system) using a septum-sealed 10 ml glass tube. Dichloro (*p*-cymene)ruthenium (II) dimer (0.0612 g, 0.1 mmol, Aldrich) and 4,7-diphenyl-1,10-phenanthroline (0.233 g, 0.7 mmol, Aldrich) in 5 ml of DMF were subjected to a 300 W microwave source at 200 °C for 5 min. After cooling the reaction tube, the complex was precipitated using 2 ml dichloromethane and 5 ml diethyl ether. The isolated bright red-orange solid was further re-crystallized using dichloromethane and diethyl ether, yielding (0.194 g) 83.2%. 1H NMR (500 MHz, DMSO-D6) δ (ppm): 7.61–7.71 (m, 24H), 7.84–7.85 (d, 6H), 8.29 (s, 12H), 8.36–8.37 (d, 6H). LC-MS (API-ES): *m/z* C72H48Cl2N6Ru Calcd 1168.2, found [M+] 1168.2. Elemental analysis calcd (%) for C40H44IN3O3: C, 73.96; H, 4.14; N, 7.19; found: C, 73.97; H, 4.15; N, 7.18.
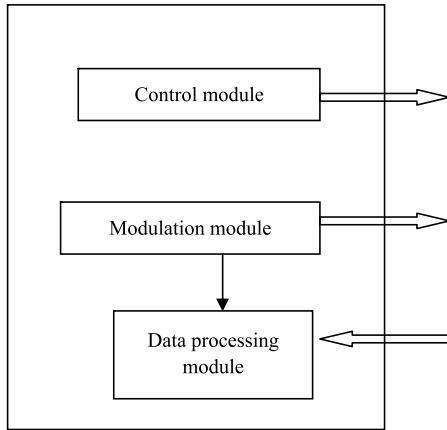
2.3.2. Film surface modification and sensor performance. For a dissolved oxygen sensor to be of practical value, a high over-all quenching response is necessary in order to attain good sensitivity at low oxygen concentrations. Quenching response is rooted in the combination of the low concentration oxygen in water and the hydrophilic nature of the sol–gel film surface. TEOS-based films have a high surface coverage of silanol (SiOH) groups [14], which facilitate water adsorption on the surface of the film, making it highly hydrophilic. However, a hydrophobic film surface is considered to be the best reinforcing DO quenching process. Fortunately, this can be achieved with the use of modified silica precursors. We used modified precursor, MTEOS, to replace the majority of the surface SiOH groups with SiCH$_3$ groups in the sol–gel film fabrication process. In order to optimize the ratio of MTEOS and TEOS, a systematic study was carried out using MTEOS in environments of 100% oxygen and 100% nitrogen. A number of sols were fabricated with increasing ratios of MTEOS to TEOS, ranging from sols with 100% TEOS to sols with 100% MTEOS. Films were fabricated as described earlier and their DO quenching responses in the gas phase were measured. As can be seen from table 1, increasing the ratio of MTEOS could cause the quenching response, Q_{DO}, to increase as expected.

Optical oxygen sensors based on both fluorescence intensity and phase fluorimetric measurements of $Ru(Ph_2phen)_3Cl_2$

Table 1. Quenching response of TEOS and MTEOS films in the gas phase.

Sol–gel film	Q_{DO} ($\pm 2\%$) %
TEOS	27
MTEOS–TEOS (1:1)	48
MTEOS–TEOS (2:1)	79
MTEOS–TEOS (3:1)	81
MTEOS	81

Figure 1. Schematic of system.

have been reported previously [15]. In order to establish a baseline for the oxygen response within a real water sample, preliminary measurements were made within fully oxygenated and fully de-oxygenated water, respectively. The films used for these initial measurements were MTEOS–TEOS-based at pH 1.5 and $R = 2$. The response was characterized by repeatability, high signal-to-noise ratio and good reversibility. As shown in figure 2, the response time of the sensor was very short (<10 s), the time from the maximum value to half of the maximum value is about

8 s. The quenching response, Q_{DO}, of the sensing was 87% with a standard deviation of 2%, where the film response was averaged over four readings. The over-all quenching response of the film may be characterized by the following equation:

$$Q_{DO} = \frac{I_{deoxy} - I_{oxy}}{I_{deoxy}}$$

where I_{oxy} and I_{deoxy} are the fluorescence signal from the film in fully oxygenated and fully de-oxygenated water, respectively. These results clearly indicated that the sensor material had a high sensitivity to dissolved oxygen in water.

3. Principle of the phase detection

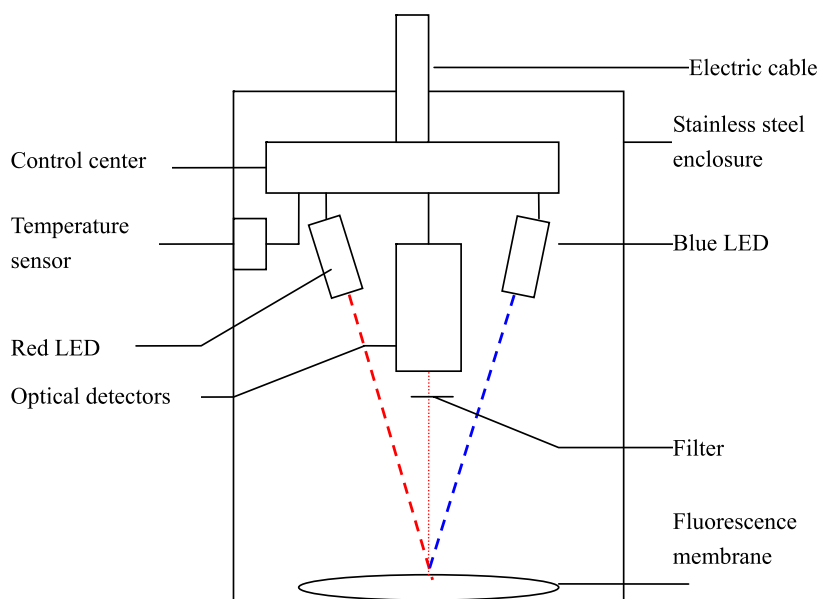The phase relationship of the sensor is given by

$$\frac{\tau_0}{\tau} = 1 + KP$$

$$\tau = \frac{\tan \phi}{2\pi f}$$

in which τ_0 represents the fluorescence lifetime in de-oxygenated water, τ represents the fluorescence lifetime for measurement in a given environment. K is the Stern–Volmer constant for the specific fluorescing material. P represents air pressure, f is the modulation frequency, ϕ is the phase of the modulation signal. The lifetime τ has a direct relationship with the phase function $\tan \phi$, which is to be the physical basis for calculating the dissolved oxygen concentration from the phase measurement.

3.1. Description of the instrument

A schematic of the system is shown in figure 1. The system contains three modules: the control module, the modulation module and the data processing module. The system uses

Figure 2. Schematic of sensor probe.

Figure 3. Photograph of the sensor.

Figure 5. Flow chart schematic for the concentration calculation.

a low power consumption MSP43f149 controller within the control module. The control module is used to control the emitting source and the reference source emission time sequence, and the modulation module is used to control the frequency of two emitting light sources. The typical frequency is modulated to 5 kHz in use. The data processing module is connected to the input measurement signal. The target signal and the reference signal are processed with a DFT algorithm and the phase of the two signals can be obtained. As the concentration of the oxygen is proportional to the phase difference, combined with the saved calibration slope/curve, the oxygen concentration can then be calculated using this module.

Figure 2 is the schematic of the sensor probe itself. A compact probe configuration was used to be compatible with the requirements of different applications. The main part of the p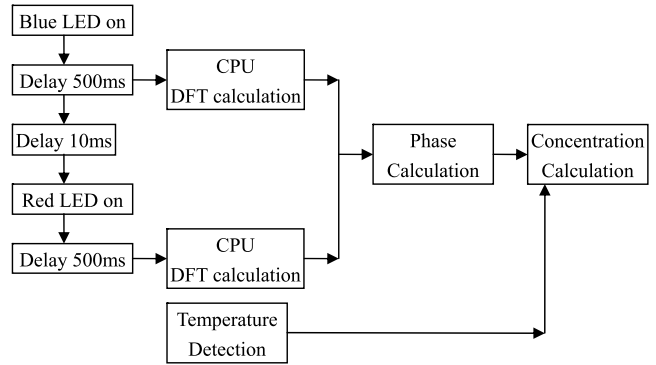robe contains the following: control center, temperature sensor, optical detectors, filter, electrical cables, and two LEDs (blue LED and red LED). All the parts (including the three modules in figure 1) are integrated into a stainless steel enclosure. The length of the probe is about 12 cm and the volume of the control unit is about 15 cm × 10 cm × 8 cm (figure 3). The control center is the most important item, because it is integrated in the probe. All the active systems, including the modulation module and the data processing module are controlled by this unit. The emitting system comprises two LEDs, which are modulated at the same frequency. The only difference between the two LEDs is the central wavelength: the central wavelengths of the red and blue LEDs (both obtained from Production of Shenzhen Weirui, China) are 620 nm and 450 nm, respectively. The current of the two pulsed LEDs is about 10 mA.

To ensure emission and detection efficiency, the divergence angle of the LEDs is limited to 5 mrad. To avoid the influence of environmental stray light and ensure a high detection accuracy, two techniques were used. First, the lights (two LEDs) were modulated at 5 kHz. Second, a narrow band filter (Shenyang Huibo, with the central wavelength 620 nm) was placed before the detector.

Figure 4 is the schematic of the electronics system. The two LEDs are modulated at 5 kHz square-wave modulation.
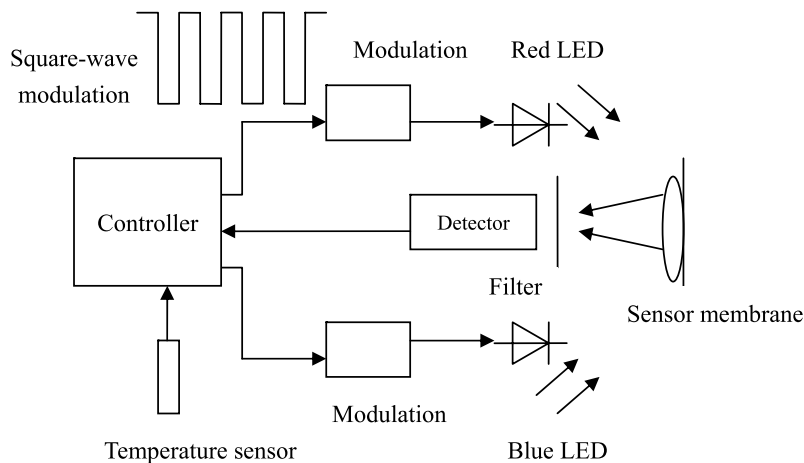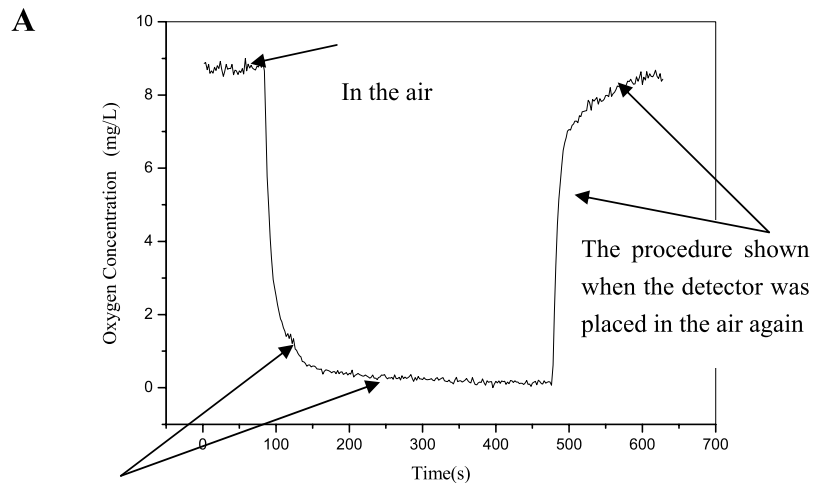

Figure 4. Schematic of the electronics system.

A

In the air

The procedure shown when the detector was placed in the air again

The procedure shown when the detector was placed in water

B

Figure 6. (A) Sensor response to different oxygen concentration and (B) application in the Xin'anhe waste water treatment plant.

The blue and red LEDs illuminate the sensor membrane at a fixed time interval. The detector receives the signal filtered by a narrow width filter effective at 620 nm. The controller is the center of the system, which is responsible for emission signal modulation, collection of temperature data and the calculation of the data. Figure 5 is the flow chart schematic for the concentration calculation. First, the blue LED is turned on (the state for the red LED is off) for 500 ms, while the controller carries out the calculation of the DFT algorithm. Then the blue LED is turned off and the red LED (the reference light source) is turned on for 500 ms, while the same DFT algorithm is executed in the controller. After data collection is complete, the phase difference can be calculated. At the same time, temperature data is collected for use as calibration data.

3.2. Sensor calibration

The solubility of oxygen in water and fluorescence films are both easily affected by the water temperature. For example, the dissolved oxygen in 0 °C water (at the standard atmosphere pressure) is about 14.62 mg l^{-1} and the dissolved oxygen in 22 °C water is about 8.74 mg l^{-1}.[4] The influence of temperature is characterized by recording the response of the sensor as a function of temperature. Then the temperature corrected calibration function was saved in the controller. When the sensor is inserted into a water sample, the effect of temperature variation can be eliminated by using the saved calibration information.

4 The Environmental Protection Industry Standards of the People's Republic of China, HJ 506-2009.

5

When the system is in an actual application, *in situ* calibration is necessary. The calibration process is shown as follows: first, the phase value in air is collected as the minimum value for calibration. Then, Na_2SO_3 is gradually added to the water sample until the solution is saturated. After waiting 20 min, the phase value in the saturated water is measured as the maximum value. The true value of the dissolved oxygen in air and in the saturated water is measured using a chemical iodometer in the laboratory. The value of the phase is a one-to-one correspondence to the true value of the linear relation as measured by the iodometric method. A two-point calibration method is used to get the linear relation between the phase value and the linear relation value.

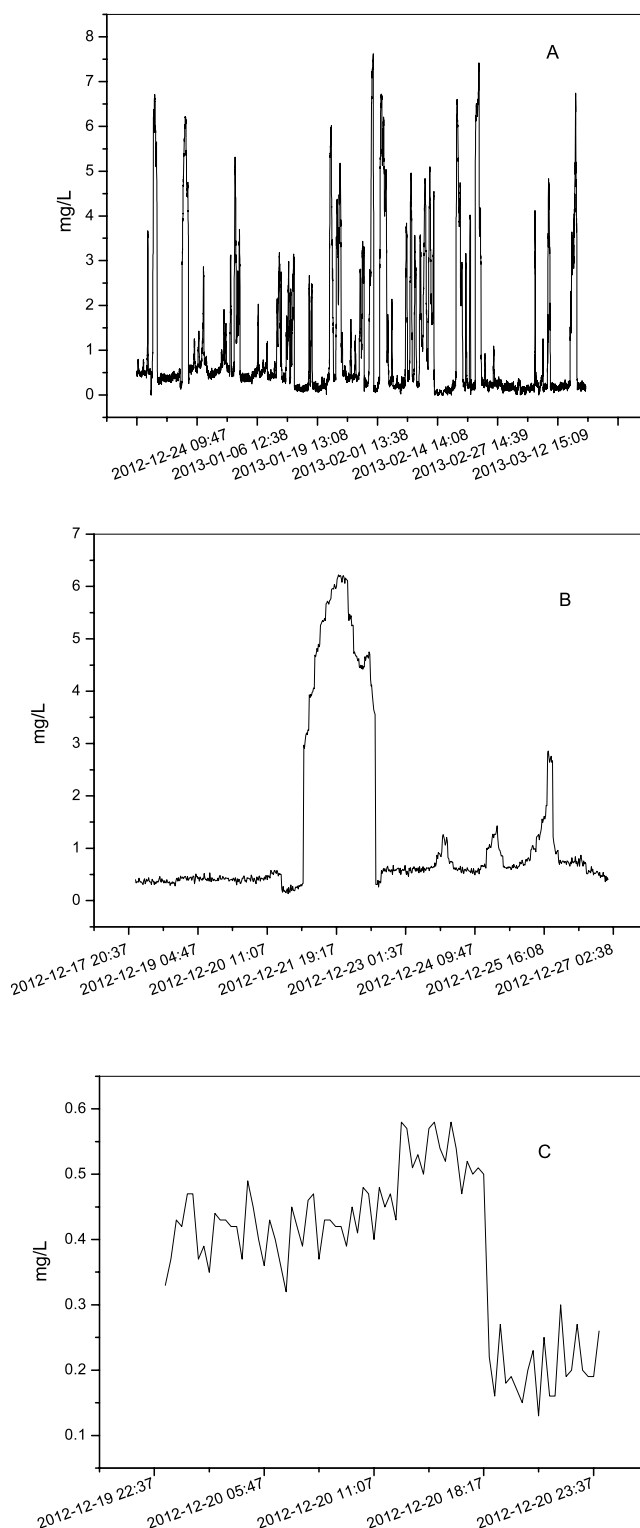## 4. Experimental results and photo-stability analysis of fluorescence film

Sensor response was tested by immersing the probe into water. In order to simulate non-air conditions, some Na_2SO_3 was added into the water. Figure 6(A) is the procedure for the DO probe testing. The procedure is as follows: the probe is placed in the air, then in the water, then out of the water again. When the probe was placed in the air, the output of the value is the concentration of the oxygen in the air. When the probe was placed in the water, the output value will quickly decrease because it is in a non-air condition. When it was pulled out of the water sample, the output value showed a rapid increase.

In order to validate the reliability of the sensor in extreme conditions, the sensor was put in the Xin'anhe wastewater treatment plant (one of the largest wastewater treatment plants in Yantai) for six months of testing. The installation position is in the aeration tank. Figure 6(B) is a photo for the sensor after six months. Figure 7(A) is part of the three month data recently taken from 12 December 2012 to 18 March 2013. Figure 7(B) is detailed data for roughly one week from 18 December 2012 to 27 December 2012. Figure 7(C) is the more detailed data for roughly one day from 00:37 to 23:07 on 19 December 2012. As shown in figure 7, there are number of dissolved oxygen fluctuations, which are closely related to the aeration rate in the aeration tank. After six months of testing, it is affirmed by the wastewater treatment plant and the market. Now, this sensor is industrialized as one of the products of Yantai Dongrun Instrument Co., Ltd.

5. Conclusion

A new DO sensor using optical methods was reviewed in this paper. It is proved to be very convenient for *in situ* and on-line water quality monitoring. Calculations of the oxygen concentration are based on the quenching of fluorescence in the presence of oxygen.

A DFT algorithm is used to calculate the phase of the opto-electrical input signal, which is linearly correlated to oxygen concentration. The emission LEDs are modulated by a square-wave 5 kHz signal and a red LED is used as the reference source to avoid an unwanted phase shift. A temperature sensor is integrated within the system and temperature compensation is completed for every

Figure 7. Sensor on-line monitoring results for about (A) three months, (B) one week and (C) one day.

measurement. In order to validate the application of the described sensor to on-line DO monitoring, experimental results are given in this paper. From the experimental data it is found that the described sensor responds very rapidly to DO concentration variations, which should make it suitable for real-time and *in situ* monitoring.

Acknowledgments

References

[1] Carritt D E and Carpente J H 1966 Comparison and evaluation of currently employed modifications of Winkler method for determining dissolved oxygen in seawater—a NASCO report *J. Mar. Res.* **24** 286–381

[2] Chen G 2004 Electrochemical technologies in wastewater treatment *Sep. Purif. Technol.* **38** 11–41

[3] Ishiji T and Kaneko M 1995 Photoluminescence of pyrenebutyric acid incorporated into silicone film as a technique in luminescent oxygen sensing *Analyst* **120** 1633–8

[4] Draxler S and Lippitsch M E 1996 Time-resolved fluorescence spectroscopy for chemical sensors *Appl. Opt.* **35** 4117–23

[5] McDonagh C, Kolle C, McEvoy A K and Dowling D L 2001 Phase fluorometric dissolved oxygen sensor *Sensors Actuators* B **74** 124–30

[6] Holst G A, Koster T, Voges E and Lubbers D W 1995 FLOX—an oxygen-flux-measuring system using a phase-modulation method to evaluate the oxygen-dependent fluorescence lifetime *Sensors Actuators* B **29** 231–9

[7] Xiong X, Xiao D and Choi M M F 2006 Dissolved oxygen sensor based on fluorescence quenching of oxygen-sensitive ruthenium complex immobilized on silica–Ni–P composite coating *Sensors Actuators* B **117** 172–6

[8] Chu F H, Yang J J, Cai H W, Qu R H and Fang Z J 2009 Characterization of a dissolved oxygen sensor made of plastic optical fiber coated with ruthenium-incorporated solgel *Appl. Opt.* **48** 338–42

[9] Chan M A, Lawless J L, Lam S K and Lo D 2000 Fiber optic oxygen sensor based on phosphorescence quenching of erythrosin B trapped in silica–gel glasses *Anal. Chim. Acta* **408** 33–7

[10] Choi M M F and Xiao D 2000 Single standard calibration for an optical oxygen sensor based on luminescence quenching of a ruthenium complex *Anal. Chim. Acta* **403** 57–65

[11] Chuang H and Arnold M A 1998 Linear calibration function for optical oxygen sensors based on quenching of ruthenium fluorescence *Anal. Chim. Acta* **368** 83–9

[12] Bolink H J, Cappelli L, Coronado E, Gratzel M and Nazeeruddin M K 2006 Efficient and stable solid-state light-emitting electrochemical cell using tris (4,7-diphenyl-1,10-phenanthroline) ruthenium (II) hexafluorophosphate *J. Am. Chem. Soc.* **128** 46–7

[13] Brinker C J and Scherer G W 1990 *Sol–Gel Science: The Physics and Chemistry of Sol–Gel Processing* (New York: Academic)

[14] Hench L L and West J K 1990 The sol–gel process *Chem. Rev.* **90** 33–72

[15] McEvoy A K, McDonagh C M and MacCraith B D 1996 Dissolved oxygen sensor based on fluorescence quenching of oxygen-sensitive ruthenium complexes immobilized in sol–gel-derived porous silica coatings *Analyst* **121** 785–8